Ground- and Excited-State Tautomerism in Anionic 2-(6′-Hydroxy-2′-pyridyl)benzimidazole: Role of Solvent and Temperature†

M. Carmen Ríos Rodríguez, Manuel Mosquera,* and Flor Rodríguez-Prieto*

Departamento de Química Física, Facultade de Química, Universidade de Santiago de Compostela, E-15782 Santiago de Compostela, Spain

Received: January 5, 2001; In Final Form: February 26, 2001

By means of UV absorption and fluorescence spectroscopy, we found that the ground- and excited-state behavior of the monoanion of 2-(6′-hydroxy-2′-pyridyl)benzimidazole (**1**) is solvent dependent. In basified protic solvents (water, ethanol), a tautomeric equilibrium exists in the ground state between the monoanion deprotonated at the hydroxyl group (normal anion) and its keto tautomer, resulting from a proton transfer from the benzimidazole N−H to the pyridine N (keto anion). In basified aprotic solvents (acetonitrile, DMSO), only the keto anion is present in the ground state. In protic solvents, the normal anion experiences in the excited state a solvent-catalyzed proton transfer (more efficient in ethanol than in water) to give the keto tautomer. The phototautomerization is temperature dependent in ethanol, the process not taking place at low temperature. We propose that in the ground state, most of the normal anion molecules are hydrogen-bonded to ethanol in such a way that the structure of the solvate is inappropriate to tautomerize. Upon excitation of the normal anion, a two-step tautomerization occurs. The first step involves a solvent rearrangement to form a cyclical solvate with the normal anion, and the second step implies a very fast multiprotonic transfer within the solvate to give the keto anion.

Introduction

It is known that molecules having acidic or basic groups may undergo an excited-state proton-transfer process as a result of the increase of acidity and basicity of those groups upon excitation. If a molecule possesses both an acidic and a basic group in close proximity and with the appropriate geometry for an intramolecular hydrogen bond to be formed, an excited-state intramolecular proton-transfer process (ESIPT) may take place, the result being a phototautomerization of the original molecule.[1−4] If the groups involved in the proton transfer are far from each other or cannot adopt the adequate geometry to form an intramolecular hydrogen bond, an excited-state proton-transfer process (ESPT) can still take place, assisted by molecules (frequently the solvent) with both hydrogen-bond accepting and donating abilities,[4] these molecules acting as bridges between the acidic and the basic site.

Phototautomerization by solvent-assisted proton transfer has been detected for various types of molecules. Among them is a group constituted by molecules exhibiting an ESPT from an N−H group to an aromatic nitrogen. This kind of ESPT processes has been reported to occur assisted by protic species for 7-azaindole (7-AI),[4−17] 1-azacarbazole (1-AC)[14,18] and derivatives,[19−22] 2-(2′-pyridyl)indoles,[17,19,22−25] and 2-(2′-pyridyl)-benzimidazole.[26−28] Moreover, this ESPT also takes place within the dimers of 1-AC[29,30] and 7-AI,[5,31−36] 7-azaindole dimers having been proposed as a model of DNA base pair for the investigation of photoinduced mutagenesis.[34−36] The mechanism of the phototautomerization of these molecules in bulk alcohols and water remains an issue of discussion. Most of the authors propose, based on the fact that at low temperature the excited-state tautomerization is excluded or hardly takes place, that in alcohols and water, the excited normal form of 7-AI[6−9] and 2-(2′-pyridyl)indoles[25] does not have the adequate solvation (1:1 cyclical complex) for a fast solvent-assisted ESPT to occur. They argue that if the excited normal form were "correctly" solvated a tautomerization process as rapid as that observed in the dimers ($k = 10^{12}$ s^{-1} for the 7-AI dimer[33]) would take place. Furthermore, the low-temperature fluorescence data for 7-AI[7] and pyridylindoles[25] in alcohols reveal that the value of the observed activation energy for the tautomerization process corresponds to that of the solvent viscous flow activation energy. A two-step mechanism for the tautomerization is proposed,[6−9,25] in which the excited species, with an inappropriate solvation, reorganizes to yield a 1:1 cyclical complex, followed by a fast proton transfer in this complex to give the tautomer. From this model it is seen that the reaction is controlled by the solvent reorganization at low temperature, and by the proton-transfer process at high temperature. Moreover, a less efficient tautomerization in water than in alcohols is observed for 7-AI. Various authors[8−10] attribute this difference to the formation of solvates with water that block the phototautomerization due to the structure of water, consisting of water molecule chains (both the N−H and the pyridine N are independently solvated by water chains). Recently, Mente et al.[14] proposed a different mechanism for the phototautomerization based on classical Monte Carlo and molecular dynamics simulations in complexes of 1-AC and 7-AI with alcohols and water. They conclude that the solvation dynamics is as fast in water as in alcohols, and propose that the excited-state reaction is not controlled by solvent dynamics effects, but by the fraction of molecules having the "reactive" geometry.

We have recently shown[37] that the monocations of 2-(6′-hydroxy-2′-pyridyl)benzimidazole (**1**) and 1-methyl-2-(6′-hydroxy-2′-pyridyl)benzimidazole (**2**), see Scheme 1, protonated at the benzimidazole N(3), experience in acetonitrile an alcohol-assisted ESIPT from the hydroxyl group to the pyridine N

† This work was presented at the PP2000 in Costa do Estoril, Portugal, honoring Professor Ralph Becker's contributions.

* Corresponding authors.

10.1021/jp010053i CCC: $20.00
Published on Web 05/02/2001

SCHEME 1: Molecular Structures of 1 and 2, the Anion of 2, the Possible Monoanions of 1 (NA, KA and EA), and the Dianion of 1 (DA)

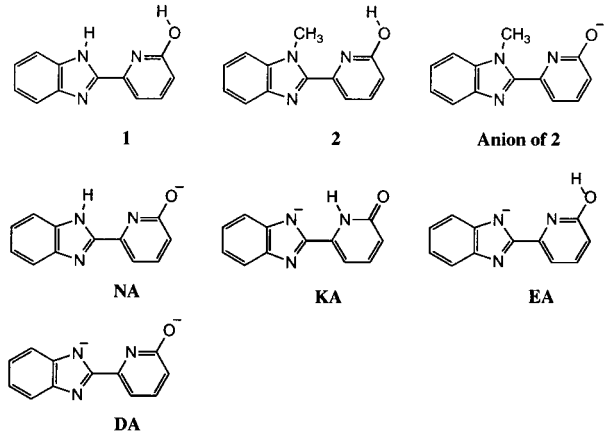

induced by the increase of basicity at the pyridine N upon excitation. We have detected this increase of basicity at the pyridine N in the excited state for the related molecule 2-(3′-hydroxy-2′-pyridyl)benzimidazole (HPyBI)[38] and its derivative methylated at the benzimidazole N(1)[39] in aqueous solution. Thus, the enol monocations, protonated at the benzimidazole N(3), tautomerize in the excited state to yield the keto cation, protonated at the pyridyl N, in a two-step process involving protonation at the pyridyl N and deprotonation at the hydroxyl group. Furthermore, the derivative 2-(2′-pyridyl)benzimidazole (2PBI), without a hydroxyl group, experiences in neutral ethanolic solution[26,27] an alcohol-catalyzed ESPT from the benzimidazole N−H to the pyridine N to give a phototautomer and protonates at the pyridyl nitrogen in neutral aqueous solution,[28] this showing again the increase of basicity at the pyridyl N experienced by this type of molecule in the excited state.

In this work we have studied the behavior of the monoanion of **1** in both protic and aprotic solvents. The aim of this research was to study the tautomerism of this monoanion, detected in both the ground and the first-excited singlet state. We investigated the mechanism of the tautomerization in the excited state, finding that a solvent-assisted excited-state proton transfer from the benzimidazole N−H to the pyridyl N can take place for the monoanion of **1**. Compound **2** was employed as a model compound, as its monoanion has no acidic hydrogen (see Scheme 1 for the structure of the anion of **2**, the three possible monoanions of **1** and the dianion of **1**).

Experimental Section

The compounds **1** and **2** were prepared as described elsewhere.[37] Solutions were made up in double-distilled water and spectroscopy grade solvents and were not degassed. Acidity was varied with NaOH (Merck p.a.). To obtain a basified medium in nonaqueous solvents, [NaOH] = 2×10^{-4} mol dm^{-3} and [NaOH] = $(0.5 - 2) \times 10^{-4}$ mol dm^{-3} were employed in ethanol and DMSO respectively, whereas in acetonitrile the solution was saturated with NaOH. We checked by UV−vis absorption spectroscopy that all ground-state **1** and **2** were found as the monoanions under these conditions except for acetonitrile, where a small amount of neutral form was still present. All experiments were carried out at 25 °C unless otherwise stated.

pH was measured with a Radiometer PHM 82 pH meter equipped with a Radiometer Type B combined electrode except for pH > 12, for which the pH was calculated to be 14 + log[NaOH]. Acidity constants reported in this work are not thermodynamic as they have been defined in terms of concentrations. UV−vis absorption spectra were recorded in a Varian Cary 3E spectrophotometer. Fluorescence excitation and emission spectra were recorded in a Spex Fluorolog-2 FL340 E1 T1 spectrofluorometer, with correction for instrumental factors by means of a Rhodamine B quantum counter and correction files supplied by the manufacturer. Fluorescence measurements at low temperature were performed using an Oxford Instruments liquid nitrogen cryostat model 1704 with an ITC 503 control unit. Fluorescence quantum yields were measured using quinine sulfate (<3×10^{-5} mol dm^{-3}) in aqueous H_2SO_4 (0.5 mol dm^{-3}) as standard ($\phi = 0.546$).[40,41] Fluorescence lifetimes were determined by single-photon timing in an Edinburgh Instruments CD-900 spectrometer equipped with a hydrogen-filled nanosecond flashlamp and the reconvolution analysis software supplied by the manufacturer. This procedure involves convoluting a theoretical model, representing the kinetics of the measured data, with an instrument response function and then comparing this to the measured decay data. In those cases where lifetimes close to the detection limit of our equipment (0.2 ns) were obtained, a global analysis of the fluorescence decay data at several wavenumbers was performed to minimize the error in the short lifetime.

PM3 semiempirical calculations were performed with Hyperchem software version 5.0. Theoretical equations were fitted to experimental data by means of a nonlinear weighted least-squares routine based on the Marquardt algorithm.

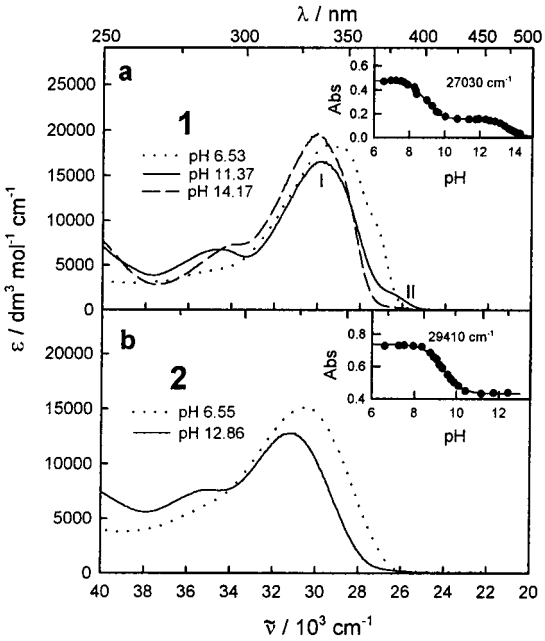

Figure 1. Absorption spectra of **1** (a) and **2** (b) in neutral and basic aqueous solutions. The insets show the pH-dependence of the absorbance for **1** (upper) at 27 030 cm^{-1} and for **2** (lower) at 29 410 cm^{-1}.

Results

1. Absorption Spectra and Acid−Base Equilibria in the Ground State. The absorption spectra of **1** and **2** under neutral and basic conditions are shown in Figures 1a and 1b, respectively. Upon increasing the pH of a neutral aqueous solution of **1** and **2**, a decrease of the absorption was observed, a new spectrum being obtained at pH ∼ 11. At this pH, the absorption spectrum of **1** showed an intense band (band I) with maximum located at 29980 cm^{-1} and a weak band at around 26700 cm^{-1} (band II). In basic aqueous solution, the absorption spectrum of **2** showed a band located at 31150 cm^{-1}, similar to band I of

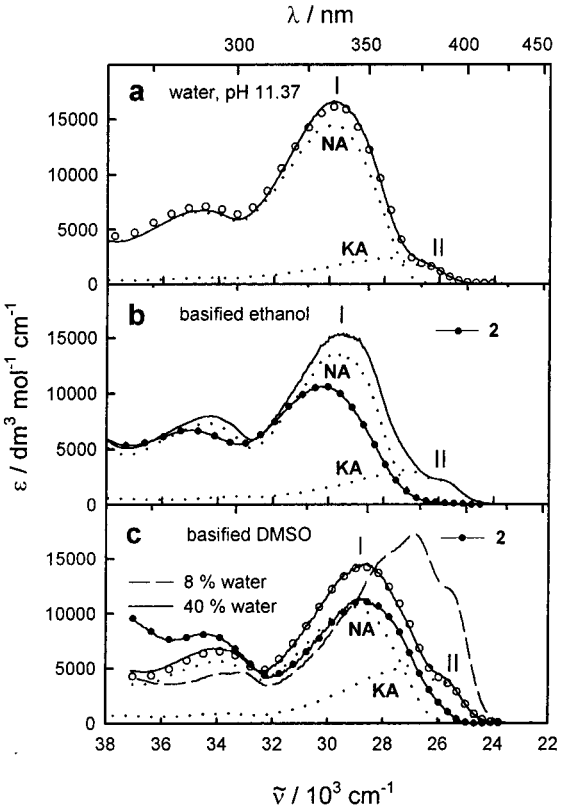

Figure 2. (a) Experimental (—) absorption spectrum of **1** in aqueous solution of pH 11.37 together with the calculated (○) spectrum obtained by fitting a linear combination of the corrected excitation spectrum of **NA** ($\tilde{\nu}_{em}$ = 25 320 cm^{-1}) and the absorption spectrum of **KA**. (b) Experimental (—) absorption spectrum of **1** in basified ethanol ([NaOH] = 1.7 × 10^{-4} mol dm^{-3}) together with the calculated contributions of **NA** and **KA**, and the absorption spectrum of **2** (− ● −) in basified ethanol ([NaOH] = 1.7 × 10^{-4} mol dm^{-3}). (c) Experimental (—) absorption spectrum of **1** in basified DMSO ([NaOH] = 1 × 10^{-4} mol dm^{-3}) with 40% water (v/v) together with the calculated (○) spectrum obtained by fitting a linear combination of the corrected excitation spectrum of **NA** ($\tilde{\nu}_{em}$ = 25 800 cm^{-1}) and the absorption spectrum of **KA**. The absorption spectra of **1** (− −) and **2** (− ● −) in basified DMSO ([NaOH] = 2 × 10^{-4} mol dm^{-3}) with 8% water (v/v) are also shown.

compound **1**, but band II was not observed for this compound. A further increase of pH induced both a blue shift in the spectrum and an increase of the maximum absorbance for **1**, a new band, peaking at 30 030 cm^{-1}, being obtained. The spectrum of **2** remained, however, unchanged. Global analysis of the absorbance−pH data at various fixed wavenumbers yielded the pK_a values 8.88 ± 0.03 and 9.362 ± 0.010 for the deprotonation of **1** and **2**, respectively, and 13.57 ± 0.03 for the second deprotonation of **1**.

The absorption spectra of **1** and **2** in basified ethanol and DMSO solutions are shown in Figures 2b and 2c. For compound **1**, the spectra obtained in basified ethanol and in basified DMSO/water solution with 40% water were similar to that measured in aqueous solution, exhibiting bands I and II, although a red shift of the bands was observed on going from water to ethanol and DMSO/water. However, in basified DMSO/water solution with 8% water the absorption spectrum was different, showing a band with vibrational structure peaking at 27 030 cm^{-1}.

2. Fluorescence Spectra and Lifetimes in Basic Media. *Aqueous Solution.* Figures 3a and 3b show the fluorescence excitation and emission spectra of **2** and **1** in basic aqueous solutions. Compound **2** exhibited in aqueous solution of pH

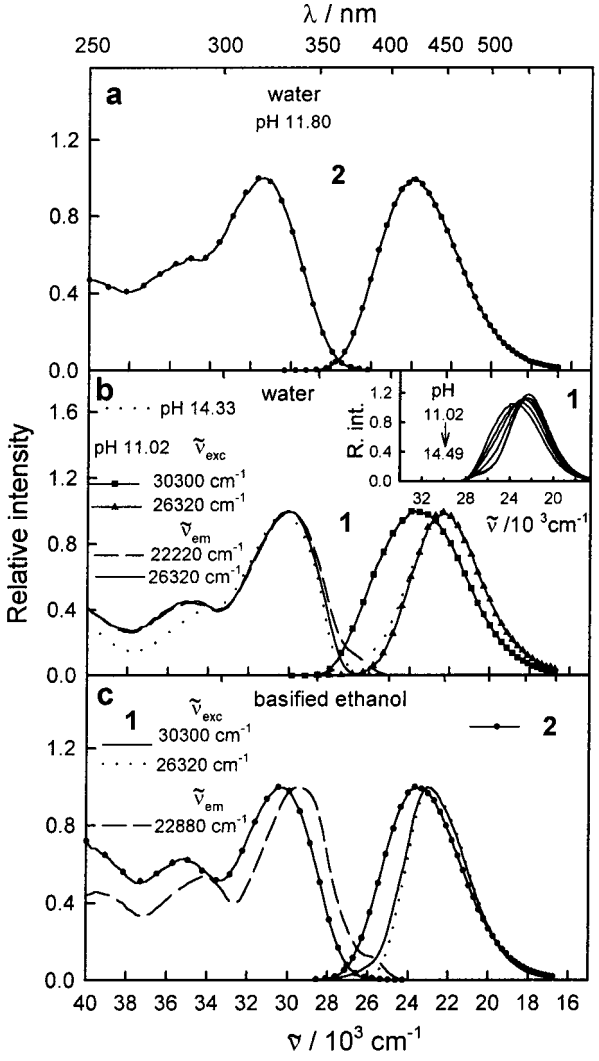

Figure 3. (a) Normalized fluorescence excitation and emission spectra of **2** in aqueous solution of pH = 11.80 ($\tilde{\nu}_{exc}$ = 31 250 cm^{-1}, $\tilde{\nu}_{em}$ = 23 530 cm^{-1}). [**2**] = 3 × 10^{-6} mol dm^{-3}. (b) Normalized fluorescence excitation and emission spectra of **1** in aqueous solution of pH = 11.02 and pH = 14.33 ($\tilde{\nu}_{em}$ = 22 220 cm^{-1}, $\tilde{\nu}_{exc}$ = 30 300 cm^{-1}). The inset shows the normalized fluorescence spectra of **1** in water with increasing pH. $\tilde{\nu}_{exc}$ = 30 300 cm^{-1}. [**1**] = 2 × 10^{-6} mol dm^{-3}. (c) Normalized fluorescence excitation and emission spectra of **1** and of **2** ($\tilde{\nu}_{exc}$ = 29 410 cm^{-1}, $\tilde{\nu}_{em}$ = 23 810 cm^{-1}) in basified ethanol. [NaOH] = 1.8 × 10^{-4} mol dm^{-3}. [**1**] = 2 × 10^{-6} mol dm^{-3}. [**2**] = 3 × 10^{-6} mol dm^{-3}.

11.80 a fluorescence band located at 23 980 cm^{-1}, which was almost independent of the excitation wavenumber (a very slight shift of the band to the red as the wavenumber decreased was observed). The fluorescence quantum yield of **2** was 0.31. The excitation spectrum showed a maximum at 31 400 cm^{-1}, almost coincident with the absorption spectrum.

Both the excitation and the emission spectra of **1** at pH 11.02 depended on the monitoring wavenumber. Under excitation at 30 300 cm^{-1} (band I), a fluorescence band peaking at 23 890 cm^{-1} was obtained, showing a quantum yield of 0.57. Excitation at 26 320 cm^{-1} (band II) led to an emission band with maximum at 22 170 cm^{-1} and a fluorescence quantum yield of 0.30. The excitation spectrum obtained at $\tilde{\nu}_{em}$ = 21 050 cm^{-1} was very similar to the absorption spectrum, with maximum at 30 030 cm^{-1} and a weak band at ∼27 000 cm^{-1}. This weak band did not appear in the excitation spectrum obtained at $\tilde{\nu}_{em}$ = 26 320 cm^{-1}. A further increase of pH induced a red shift in the emission spectrum of **1** (see inset in Figure 3b). The spectrum obtained at pH > 14 coincided with the emission band obtained

TABLE 1: Fluorescence Decay Times τ and Associated Amplitudes Ratio a_1/a_2 of 2 in Various Basified Solvents[a] at 298 K

solvent	$\tilde{\nu}_{exc}/cm^{-1}$	$\tilde{\nu}_{em}/cm^{-1}$	τ_1/ns	τ_2/ns	a_1/a_2	χ^2
water, pH 11.37	31 250	26 320[c]	2.91 ± 0.10	1.9 ± 0.3	1.9	1.07
	31 250	25 000[c]	2.91 ± 0.10	1.9 ± 0.3	1.8	1.15
	31 250	22 730[c]	2.91 ± 0.10	1.9 ± 0.3	3.7	1.01
	31 250	21 740[c]	2.91 ± 0.10	1.9 ± 0.3	14	1.11
ethanol, [NaOH] = 2.5×10^{-3} mol dm^{-3}	31 250	26 320[c]	4.41 ± 0.14	1.9 ± 0.6	2.1	1.10
	31 250	24 390[c]	4.41 ± 0.14	1.9 ± 0.6	3.8	1.00
	31 250	22 730[c]	4.41 ± 0.14	1.9 ± 0.6	3.4	1.08
	31 250	21 740[c]	4.41 ± 0.14	1.9 ± 0.6	3.4	1.09
acetonitrile[b]	29 410	22 220	5.40 ± 0.06	2.70 ± 0.06	1.4	1.16
DMSO, [NaOH] = 4×10^{-3} mol dm^{-3}	30 300	23 810	7.07 ± 0.02	2.30 ± 0.07	1.7	1.11
(9% water)	30 300	22 220	7.15 ± 0.02	2.18 ± 0.13	5.9	1.01

[a] [**2**] = $1-3 \times 10^{-5}$ mol dm^{-3}. [b] A saturated solution of NaOH in acetonitrile was employed. [c] Results of the global analysis of the decay data collected at the indicated wavenumbers.

TABLE 2: Fluorescence Decay Times τ and Associated Amplitudes Ratio a_{NA}/a_{KA} of 1 in Various Basified Solvents[a] at 298 K (lifetimes with negative amplitude in parentheses (−))

solvent	$\tilde{\nu}_{exc}/cm^{-1}$	$\tilde{\nu}_{em}/cm^{-1}$	τ_{NA}/ns	τ_{KA}/ns	a_{NA}/a_{KA}	χ^2
water, pH 11.04	30 300 (band I)	25 000[c]	2.88 ± 0.04	2.22 ± 0.08	15	1.16
	30 300 (band I)	23 810[c]	2.88 ± 0.04	2.22 ± 0.08 (−)	−2.1	1.08
	30 300 (band I)	22 220[c]	2.88 ± 0.04	2.22 ± 0.08 (−)	−1.4	1.11
ethanol, [NaOH] = 1.8×10^{-4} mol dm^{-3}	30 300 (band I)	24 390[c]	0.67 ± 0.12 (−)	2.30 ± 0.05	−0.31	1.15
	30 300 (band I)	23 530[c]	0.67 ± 0.12 (−)	2.30 ± 0.05	−0.55	1.13
	30 300 (band I)	22 220[c]	0.67 ± 0.12 (−)	2.30 ± 0.05	−0.70	0.98
	30 300 (band I)	21 280[c]	0.67 ± 0.12 (−)	2.30 ± 0.05	−0.73	1.06
	26 310 (band II)	22 220		2.273± 0.003		1.12
acetonitrile[b]	27 030	23 260	3.98 ± 0.08	1.70 ± 0.02	0.074	1.08
DMSO, [NaOH] = 3×10^{-4} mol dm^{-3}	27 780	23 810	5.80 ± 0.10	1.989 ± 0.010	0.047	1.00
(8% water)	27 780	22 220	5.74 ± 0.12	1.994 ± 0.009	0.037	0.98
	27 780	21 280	5.63 ± 0.13	1.988 ± 0.010	0.036	1.01
DMSO, [NaOH] = 5×10^{-5} mol dm^{-3}	29 410 (band I)	25 000[c]	4.93 ± 0.18	2.1 ± 0.5	2.8	1.07
(40% water)	29 410 (band I)	24 390[c]	4.93 ± 0.18	2.1 ± 0.5	2.6	1.07
	29 410 (band I)	23 810[c]	4.93 ± 0.18	2.1 ± 0.5	2.3	1.08
	29 410 (band I)	22 220[c]	4.93 ± 0.18	2.1 ± 0.5	2.0	1.08
	29 410 (band I)	21 740[c]	4.93 ± 0.18	2.1 ± 0.5	2.0	0.99
	27 030 (band II)	22 220	4.69 ± 0.05	2.26 ± 0.02	0.31	1.07

[a] [**1**] = $1-2 \times 10^{-5}$ mol dm^{-3}. [b] A saturated solution of NaOH in acetonitrile was employed. [c] Results of the global analysis of the decay data collected at the indicated wavenumbers.

at pH 11.02 under excitation in band II except for a weak emission at around 27 000 cm^{-1}.

Fluorescence lifetimes were also measured for **1** and **2** under basic conditions. The fluorescence decay of **2** at pH 11.37 was detected between 26 320 and 21 740 cm^{-1} under excitation at 31 250 cm^{-1}. A biexponential decay was obtained (Table 1) with decay times of 2.91 and 1.9 ns, the amplitudes of both decay times being positives within the wavenumber range studied.

The fluorescence decay of **1** was measured in basic aqueous solution for the NaOH concentration range $1.13 \times 10^{-3} - 2.938$ mol dm^{-3} within the monitoring range 25 000−22 220 cm^{-1} under excitation at 30 300 cm^{-1}. The decays were globally fitted to a biexponential function. At pH 11.04 global analysis yielded decay times of 2.88 ns and 2.22 ns, the amplitude of the shortest decay time being negative at low wavenumbers (Table 2). At higher pH values, an almost pH-independent decay time of 2.4 ns was obtained, together with a second decay time that decreased as the NaOH concentration increased, reaching a value of 0.24 ns at [NaOH] = 2.938 M. At each pH, the longest decay time showed a positive amplitude, whereas that of the shorter decay time was negative at low wavenumbers.

Ethanolic Solutions. Figure 3c shows the fluorescence excitation and emission spectra measured for **1** in basified ethanol solution. The excitation spectrum monitored at 22 880 cm^{-1} showed bands I and II and was almost coincident with the absorption spectrum measured under the same conditions. The fluorescence spectrum measured under excitation in band I showed its maximum at 23 070 cm^{-1} and a very weak shoulder at around 26 000 cm^{-1}, the fluorescence quantum yield being 0.58. The emission spectrum obtained by exciting in band II (fluorescence quantum yield of 0.54) was very similar, but the shoulder at 26 000 cm^{-1} was absent. Compound **2** showed in basified ethanol similar spectral features as those observed for this molecule in basified aqueous solution. Both the excitation and the emission spectra were red shifted with respect to those obtained in basic aqueous solution, a fluorescence quantum yield of 0.46 being obtained.

The fluorescence decay of **2** in basified ethanol was biexponential (Table 1) within the range 26 320−21 740 cm^{-1}, with decay times of 4.41 and 1.9 ns and positive amplitudes. Compound **1** showed also a biexponential decay (Table 2) between 24 390 and 21 280 cm^{-1} under excitation in band I, decay times of 2.30 ns and 0.67 ns being obtained. The shorter decay time exhibited negative amplitude. Excitation of **1** in band II led to a monoexponential decay with a lifetime of 2.27 ns.

The fluorescence spectra of **1** and **2** were measured in basified ethanol within the temperature range 165−295 K under excitation at 30 300 cm^{-1} (Figures 4a and 4b). For both **1** and **2**, the emission spectrum shifted to the blue as the temperature decreased, the shift being larger for **1** than for **2**. Furthermore, the excitation spectrum of **1** showed a smaller contribution of band II upon cooling the sample, only band I being observed at $T < 200$ K.

The fluorescence decay was measured for both compounds in basified ethanol under excitation at 30 300 cm^{-1} within the

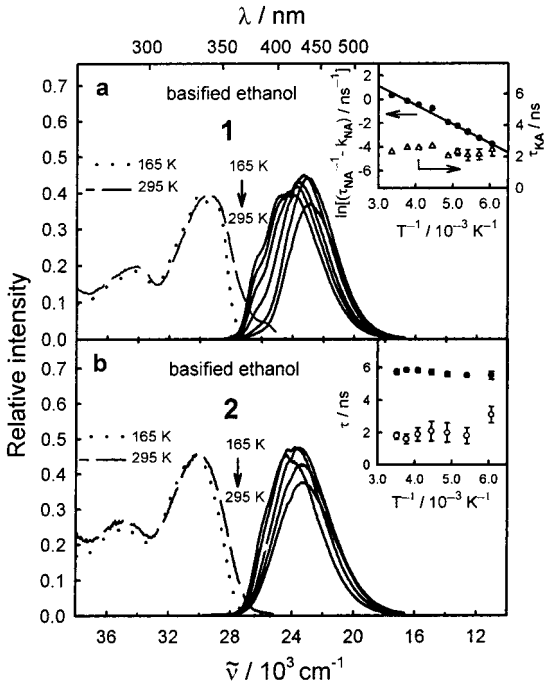

Figure 4. (a) Fluorescence spectra of **1** in basified ethanol in the temperature range 295−165 K together with the excitation spectrum at 165 and 295 K. $\tilde{\nu}_{em} = 24\,690$ cm^{-1}. $\tilde{\nu}_{exc} = 30\,300$ cm^{-1}. [NaOH] = 1.7×10^{-4} mol dm^{-3}. [**1**] = 5×10^{-6} mol dm^{-3}. The inset shows the temperature dependence of τ_{KA} and of $\ln[\tau_{NA}^{-1} - k_{NA}]$ for **1**. τ_{NA} and τ_{KA} were obtained from the triexponential global fit of the fluorescence decay of **1** in basified ethanol ([NaOH] = 1.7×10^{-4} mol dm^{-3}) between 26 320 and 22 220 cm^{-1} under excitation at 30 300 cm^{-1}. [**1**] = 3×10^{-5} mol dm^{-3}. (b) Fluorescence spectra of **2** in basified ethanol in the temperature range 295−165 K together with the excitation spectrum at 165 and 295 K. $\tilde{\nu}_{em} = 24\,390$ cm^{-1}. $\tilde{\nu}_{exc} = 30\,300$ cm^{-1}. [NaOH] = 1.7×10^{-4} mol dm^{-3}. [**2**] = 6×10^{-6} mol dm^{-3}. The inset shows the temperature dependence of the main decay times τ_1 and τ_2 obtained from the triexponential fit of the fluorescence decay of **2** in basified ethanol ([NaOH] = 1.7×10^{-4} mol dm^{-3}) at 25 000 cm^{-1} and at 22 220 cm^{-1} under excitation at 30 300 cm^{-1}. [**2**] = 4×10^{-5} mol dm^{-3}.

temperature range 165−298 K at 25 000 and 22 220 cm^{-1} for **2** and between 26 320 and 22 220 cm^{-1} for **1**. The decays were globally fitted to a triexponential function at low temperature, as the fit to a biexponential function showed to be of very bad quality. For compound **2**, decay times of 5.5 ns, 2 ns and ∼1 ns were obtained, these values showing hardly any dependence with *T* (see inset in Figure 4b). Furthermore, the shortest decay time showed a negative amplitude at both detection wavenumbers. For **1**, a decay time whose value decreased from 4.38 ns at 165 K to 0.67 ns at 298 K was obtained, together with a decay time of 2.3 ns, almost temperature independent (see inset in Figure 4a), and a third decay time of ∼1 ns. The amplitude of the 1 ns decay time was negative at $\tilde{\nu}_{em} < 26\,300$ cm^{-1}, whereas the shorter of the other two decay times showed also a negative amplitude at low wavenumbers for $T > 165$ K. Furthermore, the amplitude of the 1 ns decay time was smaller than that of the other two decay times.

Acetonitrile and DMSO Solutions. Figure 5a shows the fluorescence excitation and emission spectra of **1** in basified acetonitrile. The emission spectrum showed only one band ($\tilde{\nu}_{max} = 22\,860$ cm^{-1}) which overlapped with the excitation band ($\tilde{\nu}_{max} = 27\,140$ cm^{-1}). The excitation band showed vibrational structure and was strongly red shifted with respect to excitation band I observed in basified ethanol and water. The excitation and emission spectra were independent of the monitoring wavenumber. The fluorescence excitation and emission spectra

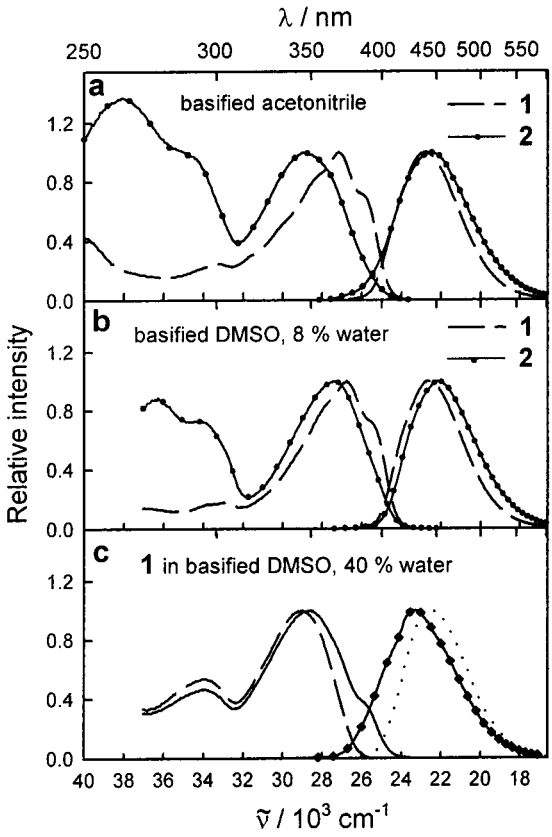

Figure 5. (a) Normalized fluorescence excitation and emission spectra of **1** ($\tilde{\nu}_{exc} = 27\,030$ cm^{-1}, $\tilde{\nu}_{em} = 23\,250$ cm^{-1}) and of **2** ($\tilde{\nu}_{exc} = 28\,750$ cm^{-1}, $\tilde{\nu}_{em} = 22\,220$ cm^{-1}) in basified acetonitrile. [**1**] = 3×10^{-6} mol dm^{-3}. [**2**] = 5×10^{-6} mol dm^{-3}. (b) Normalized fluorescence excitation and emission spectra of **1** ($\tilde{\nu}_{exc} = 27\,030$ cm^{-1}, $\tilde{\nu}_{em} = 22\,220$ cm^{-1}) and of **2** ($\tilde{\nu}_{exc} = 27\ 780$ cm^{-1}, $\tilde{\nu}_{em} = 20\,830$ cm^{-1}) in basified DMSO with 8% water (v/v). [NaOH] = 2×10^{-4} mol dm^{-3} for **1** and 4×10^{-4} mol dm^{-3} for **2**. [**1**] = 3×10^{-6} mol dm^{-3}. [**2**] = 5×10^{-6} mol dm^{-3}. (c) Normalized fluorescence excitation and emission spectra of **1** in basified DMSO with 40% water (v/v) (— $\tilde{\nu}_{em} = 21\,160$ cm^{-1}, – – $\tilde{\nu}_{em} = 25\,800$ cm^{-1}, –◆– $\tilde{\nu}_{exc} = 31\,250$ cm^{-1}, ····· $\tilde{\nu}_{exc} = 25\,640$ cm^{-1}). [NaOH] = 5×10^{-5} mol dm^{-3}. [**1**] = 3×10^{-6} mol dm^{-3}.

of **2** in basified acetonitrile overlapped to a lesser extent than those of **1**, and were both independent of the monitoring wavenumber. The fluorescence decays of **2** and **1** in basified acetonitrile were biexponential (Tables 1 and 2).

The fluorescence spectra of **1** and **2** in basified DMSO with 8% water (Figure 5b) showed the same features as those exhibited by these compounds in basified acetonitrile. The fluorescence quantum yields were 0.47 and 0.53 for **1** and **2**, respectively. The fluorescence decay of **1**, measured under excitation at 27 780 cm^{-1}, was biexponential within the range 23 810−21 280 cm^{-1} (Table 2). A biexponential decay was also obtained for **2** (Table 1). The fluorescence spectra of **1** in a basified DMSO solution with 40% water content are shown in Figure 5c. The excitation spectrum monitored at 20 830 cm^{-1} showed, as in water and ethanol, bands I and II. Excitation at 31 250 cm^{-1} (band I) led to a fluorescence band located at 23 280 cm^{-1} with quantum yield 0.60, whereas excitation at 25 640 cm^{-1} yielded a band peaking at 22 520 cm^{-1}, with quantum yield 0.53. The fluorescence decay monitored within the range 25 000−21 740 cm^{-1} under excitation at 29 410 cm^{-1} was biexponential with decay times of 4.93 and 2.1 ns, the main contribution to the decay being that of the longer decay time (Table 2). Under excitation at 27 030 cm^{-1} (band II) and monitoring wavenumber of 22 220 cm^{-1}, a biexponential decay

was also obtained with decay times of 4.69 and 2.26 ns. The main contribution to the global decay corresponded however in these conditions to the shorter decay time.

Discussion

1. Interpretation of the Absorption Spectra of 1 and 2 in Basified Solvents: Tautomeric Equilibria in the Ground State. As can be observed in Figure 2, the absorption spectra obtained for **1** in aqueous solution of pH 11.37, basified ethanol and basified DMSO with 40% water, exhibited bands I and II. However, in basified acetonitrile and DMSO with only 8% water (Figure 2c), a different structured band was observed. Compound **2** showed in this wavenumber region a single absorption band similar to band I of **1** in all the solvents studied (Figures 1b, 2b, and 2c). These results seem to indicate that for compound **1** more than one monoanion coexist in the ground state in basified solutions, their relative proportions depending on the solvent.

Compound **2** has only one acidic hydrogen, located at the hydroxyl group. Hence, dissociation of **2** leads to the monoanion deprotonated at the hydroxyl group (Scheme 1). For compound **1**, however, three possible tautomeric structures for the monoanion can be drawn, the normal anion (**NA**) deprotonated at the hydroxyl group, its keto tautomer (**KA**) resulting from a proton transfer from the benzimidazole N−H to the pyridyne N and the enol anion (**EA**) deprotonated at the benzimidazole N−H (Scheme 1). PM3 semiempirical calculations on these three monoanions showed that, in the gas phase, **KA** is the most stable structure for the monoanion. The energy levels of **NA** and **EA** were calculated to be, respectively, 6.0 and 12.6 kcal mol^{-1} higher than that of **KA**.

The energy levels of **NA**, **KA**, and **EA** in solution are not known, but the experimental results support the idea that the enol anion **EA** is also in solution the most unstable form. We know that the pK_a value for the deprotonation of the benzimidazole N−H (the same H involved in the deprotonation of **1** to give **EA**) is 12.05 for the related compound, with no hydroxyl group, 2-(2′-pyridyl)benzimidazole,[28] whereas the pK_a values for the deprotonation of the OH group in the similar compounds 2-(3′-hydroxy-2′-pyridyl)benzimidazole (HPyBI)[42] and 2-(2′-hydroxyphenyl)benzimidazole[43] are 8.57 and 8.83, respectively. On the other hand, compound **2**, which can only deprotonate at the OH group, shows a pK_a value of 9.36. The existence of two monoanions for **1** causes the macroscopic acidity constant of this compound to be a combination of two microscopic acidity constants related to the dissociation processes leading to both monoanions. According to this, if **1** deprotonated both at the hydroxyl group (yielding **NA**) and at the benzimidazole N−H (to give **EA**), we would expect for this compound a higher pK_a value than that obtained for **2**. We measured for **1**, however, a pK_a value 0.5 units lower than that of **2**. It therefore seems reasonable to suppose that **1** deprotonates exclusively at the hydroxyl group, and that the changing absorption spectra of the monoanion obtained in various solvents are due to the existence of a tautomeric equilibrium between the normal anion **NA** and the keto anion **KA**, the relative proportions of the two species depending on the solvent.

The comparison of the absorption spectra of **1** and **2** in basified protic and aprotic solvents can help to identify the species responsible for the absorption bands of **1** observed in various solvents. As the anion of **2** is deprotonated at the same position as the normal anion of **1**, we expect the absorption spectra of both anions to be very similar. It is observed in Figures 1a, 1b, and 2b that the absorption spectrum of the anion of **2** in protic solvents is similar to band I of **1**. According to this, band I should be assigned to the normal anion **NA**, whereas band II, which is not observed for **2**, must correspond to the keto anion **KA**. Furthermore, the absorption spectra of **1** in basified DMSO/water with 8% water (Figure 2c) is very different from that of **2** in the same solvent mixture, indicating that the major species responsible for the absorption spectrum of **1** cannot be **NA**, and we accordingly assign it to **KA**. Consequently, we propose that in basified protic solvents, such as water and alcohols, there are two monoanions in the ground state for compound **1**: **NA**, yielding absorption band I and **KA** giving absorption band II, whereas in basified aprotic solvents, such as acetonitrile and DMSO, **KA** is the major species present. It should be noted that when an important amount of water is added to DMSO (e.g., 40%) the mixture behaves as a protic solvent, both **NA** and **KA** being present. We conclude therefore that the tautomeric equilibrium between the normal and the keto anion shifts to the keto anion in aprotic solvents.

SCHEME 2: Resonance Structures of the Normal Anion (NA) and the Keto Anion (KA) of 1

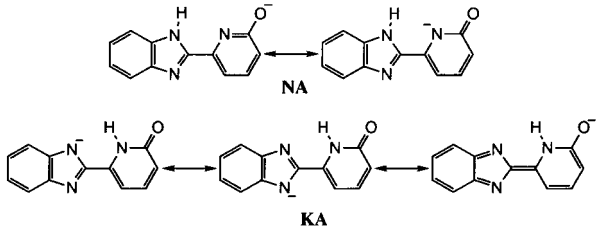

The above-mentioned results may be explained by examining the structures of the anions **NA** and **KA**. The site of protonation or deprotonation of species having more than one available position depends on the relative stability and solvation of the ions that can be formed, both the polarity and hydrogen-bonding ability of solvents affecting the stabilization of tautomers. An example of this is salicylic acid, which has been reported[44] to exist in basified polar aprotic solvents as an equilibrium between salicylate anion (the only species present in basified protic solvents) and a tautomer, deprotonated at the hydroxyl group. For the anion of **1**, according to PM3 calculations, **KA** is the more stable tautomer in the gas phase, but the relative stabilities of **KA** and **NA** may change due to differential solvation. Whereas protic solvents are known to solvate very efficiently a negative charge located at an oxygen atom, aprotic solvents, such as DMSO and acetonitrile, are inefficient in that task due to their inability to act as hydrogen bond donors.[45,46] Taking this into account, we would expect that the monoanion of **1** more favorably solvated in aprotic solvents would be that where the negative charge is more delocalized. A comparison between the resonant forms for **NA** and **KA** (Scheme 2) reveals that whereas for **NA** the negative charge is delocalized between the oxygen and the pyridyl nitrogen atoms, for **KA** the delocalization of that negative charge extends from the oxygen to the benzimidazole N, that is, between the two aromatic rings. These facts explain therefore why **KA** is the major species present in aprotic solvents. In protic solvents, **NA** should be much more stabilized, hence the comparable proportions of **NA** and **KA** observed in these solvents.

2. Excited-State Behavior of the Anion of 2. The fluorescence spectra of **2** in basified ethanol, water, acetonitrile, and DMSO are shown in Figures 3a, 3c, 5a, and 5b. In all of the solvents studied, both the excitation and the emission spectra were practically independent of the monitoring wavenumber (a very slight red shift of the emission spectrum as the excitation wavenumber decreased was observed) and, especially in water

and ethanol, showed very small overlap. The excitation spectrum coincided well with the absorption spectrum. The fluorescence decay was in all cases biexponential (Table 1), suggesting the existence of two fluorescent species. These species could be rotamers of the anion of **2**. This would explain the very slight red shift of the emission spectrum as the excitation wavenumber decreased, as the rotamers would have very similar absorption and fluorescence spectra. More information is obtained from the comparison between the absorption spectra of **1** and **2** in basified ethanol and water (Figures 1 and 2b). We observe that the molar absorption coefficient in the maximum of band I is higher for **1** than for **2**. This indicates that the conjugation between the two aromatic rings of the anion is weaker for **2** than for **1**. For compound **1**, the molar absorption coefficient of **NA** in its lowest energy band must be in fact even larger than the value read at the maximum of band I, due to the tautomeric equilibrium between **NA** and **KA**. These facts suggest that the steric hindrance of the methyl group, located at the benzimidazole N(1), causes a nonplanar anion to exist for **2**. We do not know, however, if the second rotamer is planar or another nonplanar form. Similar equilibria between planar and nonplanar rotamers were detected for related molecules, as for example 1-methyl-2-(3′-hydroxy-2′-pyridyl)benzimidazole[39] and various *N*-methyl derivatives of phenylbenzimidazoles.[47−50] With the data available, it is difficult to explain why the two rotamers have so different decay times, but the positive amplitudes obtained within the spectral region investigated indicate that they decay independently. Nevertheless, for the purpose of this work, we are only interested in **2** as a reference compound, as it does not experience a phototautomerization process.

3. Excited-State Behavior of the Anion of 1 in Aprotic Solvents. The fluorescence spectra of **1** in basified acetonitrile and DMSO (with 8% water) are shown in Figures 5a and 5b, respectively. The spectra in both solvents were very similar. The excitation spectrum showed vibrational structure and the emission spectrum showed only one band. Excitation and emission spectra overlapped and were independent of the monitoring wavenumber. The fluorescence decay was in both cases biexponential, the main component showing a decay time of 1.99 ns in DMSO and 1.70 ns in acetonitrile. The minor component showed a value of 5.7 ns in DMSO and ca. 4.0 ns in acetonitrile (Table 2). The excitation spectrum coincided well with the absorption spectrum, indicating that **KA** is the major species present in the ground state. Moreover, as the emission band overlaps with the excitation band, we must conclude that **KA** is also the major fluorescent species with a decay time of 1.99 ns in DMSO and 1.70 ns in acetonitrile. The species responsible for the long decay time is probably **NA***, which can be present in a minor amount in the ground state in these solvents.

In the basified mixture DMSO/H_2O with 40% water, **NA** and **KA** coexist in the ground state. The fluorescence excitation and emission spectra of **1** in this basified solvent mixture are shown in Figure 5c. Excitation in band II (due to **KA**) led to a single emission band that overlapped excitation band II and showed a biexponential decay with decay times of 2.26 ns (60%) and 4.69 ns (40%) (Table 2). Excitation in band I (due to **NA**) yielded a fluorescence spectrum that overlapped excitation band I and showed a blue shift with respect to that obtained under excitation in band II. The fluorescence decay under excitation in band I was biexponential, with approximately the same decay times as those obtained under excitation in band II but different contributions (2.1 ns (<18%) and 4.93 ns (>82%)). From this we conclude that excitation of **KA** leads to **KA***, this form showing a lifetime of 2.1 ns and an emission spectrum located at 22 520 cm^{-1}, whereas excitation of **NA** leads to **NA***, this species showing a lifetime of 4.9 ns and a fluorescence band shifted to the blue with respect to that of **KA***. No conversion between **NA*** and **KA*** occurs, because the amplitudes of their decay times were positive at all of the emission wavenumbers studied. Furthermore, the absorption spectrum of **1** in this solvent mixture could be satisfactorily decomposed (Figure 2c) as the sum of the contributions of **NA** (corrected fluorescence excitation band measured at $\tilde{\nu}_{em} = 25\,320$ cm^{-1}, where **KA*** shows almost no emission) and **KA** (absorption spectrum obtained in DMSO with 8% water). From this, and taking the molar absorption coefficient of **NA** in the maximum to be the same as that of the dianion **DA**, the equilibrium constant $K = [\mathbf{NA}]/[\mathbf{KA}]$ was estimated to be 1.4, indicating that both species are present in similar proportion in the ground state.

4. Excited-State Behavior of the Anion of 1 in Basified Protic Solvents: Solvent-Assisted Multiprotonic Transfer. The behavior of **1** in basified water and ethanol showed similar features. The fluorescence spectrum obtained under excitation in band I showed only one band located at 23 890 cm^{-1} in water and at 23 070 cm^{-1} in ethanol (Figure 3). In both solvents a biexponential decay was obtained under excitation in band I. One decay time showed a positive amplitude and a value of 2.30 ns in ethanol and 2.88 ns in water, and the second decay time (2.22 ns in water and 0.67 ns in ethanol) exhibited a negative amplitude (Table 2). These data point to the fact that in both solvents there is an excited-state process connecting two excited species. Excitation in band II led in water to a single band shifted to the red with respect to that obtained under excitation in band I and in basified ethanol to a band almost coincident with that obtained under excitation in band I. Furthermore, in both solvents this emission band overlapped with excitation band II. The fluorescence decay under excitation in band II could be measured only in basified ethanol, a monoexponential decay with lifetime of 2.27 ns, coincident with one of the decay times obtained under excitation in band I, being obtained. These results indicate that excitation of **KA** (band II) leads to **KA***, which shows a lifetime of 2.22 ns in water and of 2.30 ns in ethanol. Moreover, under excitation of **NA** (band I), the species **NA*** is obtained, which partly tautomerizes to yield **KA***. This tautomerization must be very efficient in basified ethanol as compared with water, because the decay time of **NA*** is only 0.67 ns in ethanol, and the fluorescence spectrum, except for a weak band located at around 27 000 cm^{-1}, which should correspond to **NA***, is almost coincident with that of **KA***. However, in basic aqueous solution, species **NA*** exhibited a decay time of 2.88 ns, the fluorescence spectrum obtained under excitation of **NA** being blue shifted with respect to that of **KA***. This means that only a small fraction of the excited **NA*** molecules lead to **KA***. We should note here that when a species experiences a transformation in the excited state, as in our case **NA*** → **KA***, and both species fluoresce, the decay time showing a negative amplitude is that with the shortest time value.[51] This is clearly illustrated by the decay times and amplitudes obtained for **1** in basified water and ethanol (Table 2). It is observed that the amplitude of the decay time associated to **NA***, the precursor of **KA***, is negative in ethanol (**NA*** is the species with the shortest decay time) and positive in water (the decay time of **KA*** is shorter than that of **NA***).

The absorption spectrum of **1** in aqueous solution of pH 11.37 could be decomposed as the sum of the contributions of **NA**

and **KA** (Figure 2a). In the fit, the absorption spectrum of **NA** was taken to be its corrected fluorescence excitation spectrum, measured at 26 320 cm^{-1} emission wavenumber, whereas that of **KA** was estimated to be the absorption spectrum of this species in DMSO with 8% water. Taking the molar absorption coefficient of **NA** in the maximum to be the same as that of the dianion **DA**, an estimated value of $K = 5.3$ was obtained. In basified ethanol, **NA*** hardly fluoresces, so that the excitation spectrum of **NA** is not known. However, assuming that the absorption spectrum of **KA** in this solvent is the same as that of this species in DMSO with 8% water and that **NA** does not absorb at low wavenumbers (as checked in basified aqueous solution), the corrected excitation spectrum of **NA** can be obtained subtracting from the experimental absorption spectrum the absorption band of **KA** in basified DMSO normalized at 25 640 cm^{-1} (Figure 2b). The absorption spectrum so obtained for **NA** is very similar to that measured for this species in basified water (Figure 2a). From the contributions of **NA** and **KA** to the absorption spectrum, and under the same assumptions made for aqueous solution, an equilibrium constant of 3.7 was calculated.

We can think of three possible mechanisms for the conversion of **NA*** into **KA*** in basified aqueous solution: (1) protonation of **NA*** at the pyridyl nitrogen leading to a neutral keto species **K***, which then deprotonates at the benzimidazole N(3) to yield **KA***; (2) deprotonation of **NA*** at the benzimidazole N(3) to yield the dianion **DA***, which in turn protonates at the pyridyl N giving also **KA***; and (3) a fast multiprotonic transfer involving a bridge of water molecules that brings the proton from the benzimidazole N to the pyridyl N.

If process 1 occurred, **NA*** would protonate to yield **K***. This species has been previously detected[45] in water and other protic and aprotic solvents under neutral conditions, showing a low fluorescence quantum yield and a lifetime of only ~0.2 ns. As **K*** is so short-lived, at pH ~ 11 the OH^- concentration is too low to compete with deactivation of **K***, thus, deprotonation **K*** → **KA*** would have to be assisted by water. If that were the case, we should observe process **K*** → **KA*** in neutral aqueous solution upon exciting directly **K**. As that deprotonation does not take place under neutral conditions, we can rule out process 1. If process 2 held, species **NA*** would deprotonate at the benzimidazole N−H to yield **DA***, which should then protonate very efficiently at the pyridyl N to yield **KA*** (note that we only detect fluorescence from **NA*** and **KA***). To decide between mechanisms 2 and 3, it would be helpful to know if **NA*** is deprotonated by OH^- and if **DA*** (when directly excited) protonates to give **KA***. To throw light on this question, we studied the influence of the [OH^-] on the fluorescence of **1** in basic aqueous solution, which will be discussed in section 4.1 below.

4.1. Influence of pH on the Fluorescence of 1 in Basic Aqueous Solution. The influence of pH on the fluorescence of **1** in basic aqueous solution was studied under excitation at 30 300 cm^{-1} (Figure 3b). It was observed that the emission band shifted to the red as the pH increased (inset in Figure 3b). At pH 14.33, a single excitation band coincident with the absorption band assigned to the dianion was obtained, indicating that **DA** is the species being excited. The fluorescence spectrum coincided, except for a weak emission band located at around 27 000 cm^{-1}, with the emission band of **KA***. Furthermore, this weak emission band overlapped with the excitation band of **DA**, indicating that **DA*** is responsible for this fluorescence. These results seem to indicate that most of the excited **DA*** molecules

SCHEME 3: Excitation and Deactivation of 1 in Basic Aqueous Solution

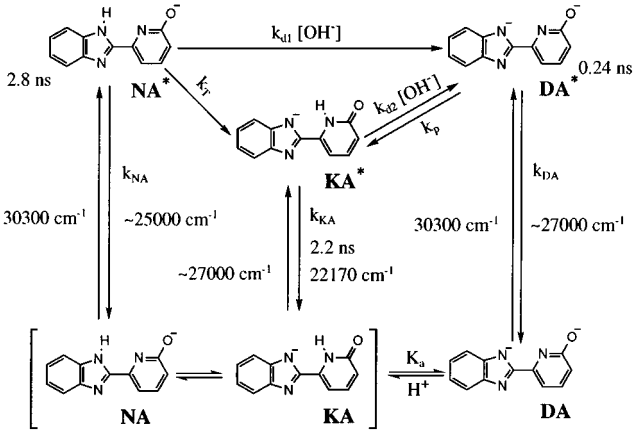

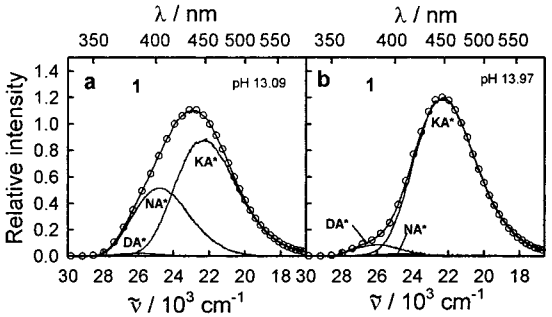

Figure 6. Experimental (—) fluorescence spectra of **1** in aqueous solution of pH = 13.09 (a) and pH = 13.97 (b) and calculated (○) spectra obtained by fitting a linear combination of the fluorescence of **NA***, **KA***, and **DA*** together with the individual contributions of these spectra. $\tilde{\nu}_{exc} = 30\,300$ cm^{-1}. [**1**] = 2×10^{-6} mol dm^{-3}.

are protonated by water at the pyridyl N to yield **KA*** (see Scheme 3). The fluorescence spectrum of **DA*** can be obtained under the assumption that this species does not fluoresce significantly at 20 000 cm^{-1}, subtracting from the emission spectrum recorded at pH 14.49 the emission band of **KA*** (obtained at pH 11.02 under excitation in band II) normalized at 20 000 cm^{-1}. Similarly, the fluorescence spectrum of **NA*** can be estimated (considering that this species hardly fluoresces at 20 000 cm^{-1}) subtracting from the emission spectrum measured at pH 11.02 under excitation in band I, the emission band of **KA*** (recorded under excitation in band II at the same pH) normalized at 20 000 cm^{-1}. All of the spectra from the series could be reproduced as a sum of the contributions of **DA***, **NA***, and **KA*** emissions according to eq 1, where C_{NA}, C_{KA}, and C_{DA} represent the contribution coefficients of **NA***, **KA***, and **DA*** to the total fluorescence, $F^{\tilde{\nu}}$, and $F^{\tilde{\nu}}_{NA}$, $F^{\tilde{\nu}}_{KA}$, and $F^{\tilde{\nu}}_{DA}$ are the pure fluorescence spectra of **NA***, **KA*** and **DA***, obtained as described above.

$$F^{\tilde{\nu}} = C_{NA}F^{\tilde{\nu}}_{NA} + C_{KA}F^{\tilde{\nu}}_{KA} + C_{DA}F^{\tilde{\nu}}_{DA} \qquad (1)$$

A satisfactory fit of eq 1 was obtained, as can be seen in Figures 6a and 6b, the pH dependence of the coefficients C_{NA}, C_{KA}, and C_{DA} being shown in Figure 7a. It is observed that the coefficient of **NA*** decreases as the pH increases, reaching a value of zero at high OH^- concentrations, whereas that of **KA*** increases (due to process **DA*** → **KA***), reaching a maximum at pH ~ 14 and decreasing at higher basicity conditions. This result, together with the fact that the coefficient of **DA*** increases with pH in all of the regions investigated, although for

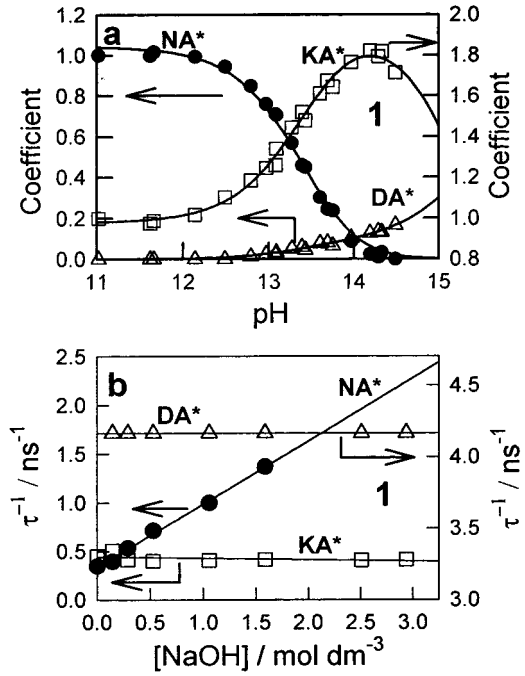

Figure 7. (a) Plot of the dependence of the relative contributions of **NA***, **KA***, and **DA*** to the fluorescence spectrum of **1** under excitation at 30 300 cm^{-1}. The solid curves are the result of fitting eqs 2−6 to the experimental data. (b) $[OH^-]$ dependence of the reciprocal of the decay times τ_{NA}, τ_{KA}, and τ_{DA} obtained from the triexponential fit of the fluorescence decay of **1** in aqueous solution. The decay times are the result of the global analysis between 25 000 and 22 220 cm^{-1}.

pH > 14 only **DA** is present in the ground state, leads us to conclude that at high pH values **KA*** deprotonates to yield **DA*** (Scheme 3).

The fluorescence decay of **1** was measured in basified aqueous solution for the NaOH concentration range 1.13×10^{-3} to 2.938 mol dm^{-3} between 25 000 and 22 220 cm^{-1} under excitation at 30 300 cm^{-1}. As a first approach, the data were fitted to a biexponential function, a decay time of 2.4 ns (almost independent of $[OH^-]$) being obtained, together with a second decay time whose value decreased as the OH^- concentration increased. At each OH^- concentration, the longest decay time showed a positive amplitude at all detection wavenumbers, whereas the shortest decay time exhibited a negative amplitude at low wavenumbers. The constant decay time of 2.4 ns, whose contribution to the global decay increased with the $[OH^-]$, corresponds to **KA***. The decay time of **NA*** decreased, however, as $[OH^-]$ increased, indicating that **NA*** is quenched by $[OH^-]$ to yield dianion **DA***. At high OH^- concentrations (>2.5 M), only **DA** is excited and, besides the decay time of 2.4 ns, corresponding to **KA***, a decay time of 0.24 ns was obtained. This short decay time must be then assigned to **DA***. It is observed that the value of the decay time of **NA*** approaches that of **DA*** as the $[OH^-]$ increases. Furthermore, the contribution of **NA*** decreased as the $[OH^-]$ increased, and the amount of **DA*** is small for all the pH range (the maximum contribution corresponds to $[OH^-] = 2.938$ M, when only **DA** is excited, see Figure 7a). As a result of this, the decay time assigned to **NA*** at intermediate pH values can be an average of the decay times of **NA*** and **DA***. To avoid this, we have fitted the data in that range to a triexponential function, keeping the decay time of **DA*** (0.24 ns) constant. The reciprocals of these decay times were then plotted against the $[OH^-]$ (see Figure 7b). A linear dependence of τ_{NA}^{-1} with $[OH^-]$ is observed, an intercept of $(3.37 \pm 0.17) \times 10^8$ s^{-1} and a slope of $(6.4 \pm 0.2) \times 10^8$ mol^{-1} dm^3 s^{-1} being obtained. From this, we conclude that species **NA*** deprotonates by OH^- to yield **DA***, the rate constant for this deprotonation process being the slope of the straight line.

The above-mentioned results allow us to analyze the mechanism of the phototautomerization process **NA*** → **KA***, which can take place directly or via **DA***. The fluorescence spectra of **1** at high pH showed that most of the **DA*** molecules are protonated by water to yield **KA*** (Figure 6b). However, at pH ∼ 11, the OH^- concentration is too low for the deprotonation of **NA*** to compete with its deactivation. As a result of this, the phototautomerization **NA*** → **KA*** must take place at this pH via the two-step process **NA*** → **DA*** → **KA***, both steps being assisted by water, or occur directly, water molecules acting as bridges between the proton donor and acceptor sites. From the fluorescence at high pH values we know that if **DA** is excited, only part of these molecules protonate in the excited state to yield **KA***, fluorescence from **DA*** and **KA*** being observed. This means that if the two-step tautomerization, via **DA***, took place at low pH values, we should detect fluorescence from **DA*** already at pH ∼ 11 (this species has a decay time of 0.24 ns, very different from those of **NA*** (2.88 ns) and **KA*** (2.4 ns)). As we have not detected any fluorescence from **DA***, and, furthermore, we have not observed this deprotonation process for the monoanions of the related molecules 2-(3′-hydroxy-2′-pyridyl)benzimidazole and 2-(2′-hydroxyphenyl)-benzimidazole in basic aqueous solution, we propose that part of the excited **NA*** molecules experience a water-assisted multiprotonic tautomerization to give **KA***. On the other hand, as the coefficient of **KA*** slightly decreases with increasing $[OH^-]$ at pH > 14 (Figure 7a), whereas that of **DA*** increases without reaching a constant value, we suppose that at high pH values part of the **KA*** molecules are deprotonated by OH^- giving **DA***. According to all of this, we propose the mechanism shown in Scheme 3 to explain the excited-state behavior of **1** in basified aqueous solution.

To test the adequacy of our model, we have deduced from the mechanism the equations describing the pH dependence of the coefficients C_{NA}, C_{KA}, and C_{DA} representing the contribution of **NA***, **KA***, and **DA*** to the total fluorescence (eqs 2−6).

$$C_{NA} = \frac{\chi_{NA} K [H^+]}{(1+K)(K_a + [H^+])\delta} \tag{2}$$

$$C_{KA} = \frac{\chi_{KA}}{\xi}\left\{\left[K_a \alpha \frac{k_p}{k_{DA}} + \frac{[H^+]}{1+K}\left(1+\frac{k_p}{k_{DA}}\right)\right]\delta + \alpha \frac{K[H^+]}{1+K}\left[\frac{k_T}{k_{NA}}\left(1+\frac{k_p}{k_{DA}}\right) + \frac{k_p}{k_{DA}}\frac{k_{d1}}{k_{NA}}[OH^-]\right]\right\} \tag{3}$$

$$C_{DA} = \frac{\chi_{DA}}{\xi}\left\{\left(1+\frac{k_{d2}}{k_{KA}}[OH^-]\right)\left[K_a\delta + \beta\frac{K[H^+]}{1+K}\frac{k_{d1}}{k_{NA}}[OH^-]\right] + \frac{k_{d2}}{k_{KA}}[OH^-]\left[\beta\frac{K[H^+]}{1+K}\frac{k_T}{k_{NA}} + \gamma\frac{[H^+]}{1+K}\delta\right]\right\} \tag{4}$$

$$\xi = (K_a + [H^+])\left(1+\frac{k_{d2}}{k_{KA}}[OH^-] + \frac{k_p}{k_{DA}}\right)\delta \tag{5}$$

$$\delta = 1 + \frac{k_T}{k_{NA}} + \frac{k_{d1}}{k_{NA}}[OH^-] \tag{6}$$

TABLE 3: Tautomeric Equilibrium Constant K for 1 in Various Basified Solvents Together with the Kinetic Parameters for the Various Excited-State Processes of 1 in Basic Aqueous Solution (Scheme 3)[a]

solvent	$K = [\mathbf{NA}]/[\mathbf{KA}]$	$10^{-8}\,k_T$	$10^{-8}\,k_{NA}$	$10^{-8}\,k_{KA}$	$10^{-8}\,k_{DA}$	$10^{-8}\,k_{d1}$	$10^{-8}\,k_{d2}$	$10^{-8}\,k_p$
DMSO/water (40% water)	1.4							
ethanol	3.7							
water	5.3	1.52	1.85	4.08	3	5.2	1.3	40

[a] The rate constants k_T, k_{NA}, k_{KA}, and k_p are given in s^{-1} and k_{d1} and k_{d2} in $mol^{-1}\ dm^3\ s^{-1}$.

In these equations, χ_{NA}, χ_{KA}, and χ_{DA} represent empirical instrumental parameters, K_a is the ground-state acidity constant of the anion to give the dianion, K is the ground-state tautomeric equilibrium constant previously defined, $\alpha = \epsilon_{NA}^{30300}/\epsilon_{KA}^{30300}$, $\beta = \epsilon_{NA}^{30300}/\epsilon_{DA}^{30300}$, $\gamma = \epsilon_{KA}^{30300}/\epsilon_{DA}^{30300}$, and ϵ_{NA}^{30300}, ϵ_{KA}^{30300}, and ϵ_{DA}^{30300} are the molar absorption coefficients of **NA**, **KA**, and **DA** at 30 300 cm^{-1} excitation wavenumber. The deactivation rate constants k_{NA}, k_{KA}, and k_{DA} of **NA***, **KA***, and **DA*** account for the radiative process and all of the possible nonradiative routes different from the proton-transfer processes (Scheme 3). Equations 2−6 were globally fitted to the experimental data of C_{NA}, C_{KA}, and C_{DA}. Some parameters were kept fixed during the fit to the values obtained from an independent measurement. Thus, $K_a = 2.7 \times 10^{-13}$ mol dm^{-3} (from the analysis of absorbance−pH data), $K = 5.3$ (from the spectral decomposition of the absorption spectrum at pH 11.37 as the sum of **NA** and **KA** contributions). Furthermore, the value of ϵ_{KA}^{30300} in water was estimated assuming that the spectrum of **KA** in water is the same as that of this species in DMSO, except for a blue shift in aqueous solution. The fit provided the value of the ratio of the rate constants k_T/k_{NA}, k_p/k_{DA}, k_{d1}/k_{NA}, and k_{d2}/k_{KA}. The goodness of the fit (Figure 7a) supports the proposed mechanism. Table 3 compiles the values obtained for the rate constants involved in the mechanism (Scheme 3), calculated from the just mentioned rate constants ratios and from the time-resolved fluorescence data as described below.

From the ratio $k_T/k_{NA} = 0.82 \pm 0.11$, k_T and k_{NA} can be obtained taking into account that the intercept of the $\tau_{NA}^{-1} - [OH^-]$ plot ($(3.37 \pm 0.17) \times 10^8\ s^{-1}$) corresponds to $k_{NA} + k_T$. According to these figures (Table 3), in the absence of tautomerization, $\tau_{NA} = k_{NA}^{-1} = 5.4 \pm 0.4$ ns, a value in keeping with that of the decay time of **NA*** in DMSO with 40% water content, a solvent mixture where **NA*** does not tautomerize. Besides, a ratio $k_T/(k_T + k_{NA}) = 0.45$ is calculated, indicating that almost half of the excited **NA*** molecules tautomerize to give **KA*** via the solvent-assisted mechanism at pH ∼ 11. Moreover, the value obtained for k_{d1} (Table 3) is in keeping with that obtained for this rate constant from the analysis of the $\tau_{NA}^{-1}-[OH^-]$ data ($(6.4 \pm 0.2) \times 10^8\ mol^{-1}\ dm^3\ s^{-1}$). Furthermore, k_{d2} is calculated from the ratio $k_{d2}/k_{KA} = 0.32 \pm 0.19\ mol^{-1}\ dm^3$ and the known value of k_{KA} (the reciprocal of the decay time of **KA***). Finally, k_p was calculated from the ratio $k_p/k_{DA} = 13 \pm 9$, taking into account that in water $\tau_{DA} = (k_{DA} + k_p)^{-1} = 0.24 \pm 0.05$ ns.

4.2. Influence of Temperature on the Fluorescence of 1 and 2 in Basified Ethanol: Mechanism for the Phototautomerization of 1. In basified ethanol, the tautomerization **NA*** → **KA*** is much faster than in water, as indicated by the short decay time and weak fluorescence of **NA*** in ethanol as compared to water. For the same reasons discussed above for water, mechanism 1 does not hold in basified ethanol. If process 2 were correct, we should observe a more efficient phototautomerization in water than in ethanol (protonation and deprotonation processes are more favored in water than in ethanol). As the opposite behavior is found, we can rule out this process.

SCHEME 4: Excitation and Deactivation of 1 in Basified Ethanol (data refer to 298 K)

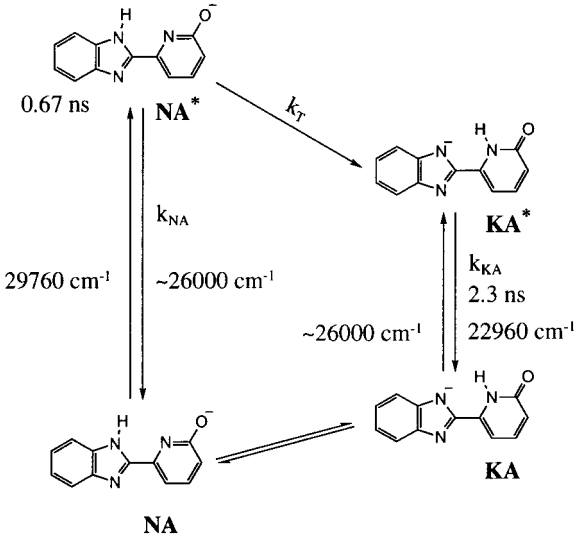

We propose a fast multiprotonic transfer involving a bridge of ethanol molecules as the mechanism for the conversion **NA*** → **KA*** (Scheme 4). To get a deeper insight into the mechanism of this process, we have studied the influence of temperature on both the fluorescence spectra and lifetimes of **1** and **2** (employed as a reference) in basified ethanol.

The fluorescence emission spectrum of **2** in basified ethanol (Figure 4b) shifted to the blue and showed a higher intensity as the temperature decreased. A triexponential function was needed to satisfactorily fit the fluorescence decay data, the quality of the fit being worse than that obtained at room temperature. Two of the decay times (5.5 and 1.8 ns) coincided with those obtained at 298 K and showed no temperature dependence (see the inset in Figure 4b). The third decay time (∼1 ns) showed a negative amplitude, whereas the other two exhibited a positive amplitude and represented the main contribution to the decay. Both the temperature-dependent spectral shift and the existence of the third decay time with negative amplitude point to the existence of a temperature-dependent solvent-relaxation process experienced by the excited anion of **2**. This could cause fluorescence from the unrelaxed state to be observed at low temperature and emission from the relaxed state to be seen at high temperature. In the intermediate region, emission from different relaxation "steps" can take place, the decay being nonexponential.

The fluorescence spectrum of **1** in basified ethanol within the temperature range 165−295 K (Figure 4a) showed also a blue shift and an increase of intensity as the temperature decreased. This shift to the blue of the emission spectrum was accompanied by the disappearance of excitation band II, only band I, assigned to **NA**, being obtained at $T < 200$ K. This indicates that **NA** is lower in energy than **KA**. Furthermore, the fluorescence decay for **1** was, as for **2**, triexponential. However, one decay time increased its value as the temperature decreased from 0.67 ns at 298 K to 4.38 ns at 165 K, and a

second decay time of 2.3 ns, independent of T, was also obtained, the shortest of these two values showing a negative amplitude at low emission wavenumbers. The third component, with a decay time of ~1 ns, showed, as for **2**, a negative amplitude at all detection wavenumbers and a low contribution to the total decay as compared to the other two decay times. The observed temperature-dependent fluorescence spectral shift, together with the presence of the negative amplitude 1 ns decay time, point to the existence of a temperature-dependent relaxation process experienced by **NA***, similar to the behavior observed for **2**. Besides that, it was observed that at 165 K species **NA*** showed a similar emission spectrum to that of the anion of **2** (species which does not tautomerize) and a decay time (4.38 ns) close to the longer decay time (5.5 ns) detected for **2**. It is then clear that the tautomerization **NA*** → **KA*** observed for compound **1** is inhibited at low temperature.

The above-mentioned results point to the fact that for **1**, species **NA*** experiences two competing processes as T is lowered, that is, a solvent-relaxation process and a phototautomerization assisted by ethanol. Kasha et al.[53] have recently reported that a competition between these two processes occurs for pyrroloquinolines. We are not going to discuss here about the solvent relaxation process, but this taking place in the same time scale as the solvent-assisted ESPT complicates the study of the latter. Nevertheless, we can still obtain information about the observed activation energy for this phototautomerization as follows.

We have shown that the excited anion of **2**, which does not tautomerize, experiences a solvent-relaxation process, and the two decay times assigned to its rotamers were shown to be temperature-independent. We then assume that the same applies for **1**, the temperature-dependence observed for the decay time of **NA*** corresponding only to the phototautomerization. Under this assumption, we have fitted the equation $\tau_{NA} = (k_{NA} + k_T(T))^{-1} = (k_{NA} + A \exp(-E_{obs}/(RT)))^{-1}$ to the experimental $\tau_{NA} - T$ data (see inset in Figure 4a). In this equation, an Arrhenius dependence of the tautomerization rate constant k_T was assumed, E_{obs} being the observed activation energy and A the preexponential factor. The fit yielded $k_{NA} = (2.05 \pm 0.09) \times 10^8\ s^{-1}$, $A = (6 \pm 4) \times 10^{11}\ s^{-1}$, and $E_{obs} = (1.41 \pm 0.12) \times 10^4\ J\ mol^{-1}$. From k_{NA}, a value of $\tau_{NA} = k_{NA}^{-1} = 4.88$ ns is obtained in the absence of tautomerization, in good agreement with the decay time measured for this species in DMSO with 40% water (where no tautomerization occurs) and with that calculated for **NA*** in basified water in the absence of tautomerization. Furthermore, the value of τ_{NA} so calculated for **1** is very close to the main decay time detected for compound **2**. Moreover, the value of the preexponential factor is in agreement with that reported for the solvent-assisted biprotonic transfer of 7-azaindole in ethanol ($9.7 \times 10^{11}\ s^{-1}$).[7] With regard to the observed activation energy, the obtained value parallels the activation energy of viscous flow of ethanol ($1.46 \times 10^4\ J\ mol^{-1}$),[25] indicating that the process is controlled by the solvent reorganization. Furthermore, we know that a solvent-catalyzed excited-state proton transfer is usually very rapid when an adequate structure of the solvate already exists in the ground state. We accordingly propose that, in the ground state, most of the **NA** molecules are hydrogen bonded to ethanol, the structure of the solvate being inadequate to tautomerize. Upon excitation of the solvate, and as a result of the increased basicity of **NA*** at the pyridyl nitrogen, a two-step tautomerization occurs. The first step involves a solvent rearrangement to form an adequate solvate with **NA***, this species yielding **KA*** in a very fast process. Unluckily, we cannot obtain from our data the number of alcohol molecules involved in the reactive solvates. Furthermore, a small proportion of **KA*** is detected at 165 K, despite **KA** being not present in the ground state. As its decay time shows a positive amplitude, these **KA*** molecules are not the result of the temperature-dependent **NA*** → **KA*** process. We then propose that a very small fraction of **NA** molecules are solvated by ethanol in the reactive geometry for the tautomerization already in the ground state, giving thus **KA*** immediately after excitation, this process being temperature independent.

To sum up, if we compare the efficiency of the solvent-assisted phototautomerization of **1** experienced by **NA*** in ethanol, water, and DMSO with 40% water, we come to the conclusion, as pointed out by Kasha and others,[8−10,53] that the structure of the solvent plays a crucial role in this process. Thus, ethanol self-aggregates to a lesser extent than water, the phototautomerization showing to be very efficient in this solvent. On the other hand, water is known to form hydrogen-bonded chains, and we observe that the water-assisted ESPT is much poorer than in ethanol. Finally, DMSO interacts strongly with water, one molecule of DMSO complexating with two water molecules. Hence, in a DMSO solution with 40% water, most of these water molecules are complexated to DMSO ($[H_2O]/[DMSO] = 2.6$). Furthermore, it is known that DMSO−water interactions are even stronger than the intermolecular association of water. As a result of this, we can easily understand why in the DMSO/water solution the phototautomerization is even more inefficient than in water, the process not taking place at all.

Conclusions

In this work we have studied the behavior of **1** and **2** in basified protic and aprotic solvents. Both the ground- and the excited-state behavior of **1** were shown to be solvent dependent.

1. In basified aprotic solvents (acetonitrile, DMSO), **1** exists in the ground state as the keto anion **KA**. Under excitation of **KA** the fluorescence of this species is observed.

2. In basified protic solvents (water, ethanol), a tautomeric equilibrium exists in the ground state between the normal anion **NA** and the keto anion **KA**, **NA** being the predominant species. Under excitation of **NA**, part of these molecules undergo a solvent-assisted tautomerization (more efficient in ethanol than in water) to yield **KA***, dual fluorescence being detected. Excitation of **KA** yields fluorescence from **KA***. Upon adding water to DMSO (40% water content), an equilibrium, similar to that observed for water and ethanol, is established between **NA** and **KA**, but no tautomerization **NA*** → **KA*** takes place.

3. Increasing the pH of a basified aqueous solution of **1** induces a quenching of **NA*** by OH^- to yield dianion **DA***, most of its molecules being protonated by water at the pyridyl nitrogen to yield the keto anion **KA***. At pH > 14, only **DA** is present in the ground state, yielding both **DA*** and **KA*** upon excitation.

4. Upon decreasing the temperature in basified ethanol, the tautomerization **NA*** → **KA*** is inhibited. The observed activation energy for this process parallels the activation energy of viscous flow of ethanol, indicating that, at low temperature, the process is controlled by the solvent reorganization. A weak fluorescence of **KA*** is detected at low temperature being due to the presence of a small fraction of **NA** molecules solvated by ethanol with the reactive geometry already in the ground state.

Acknowledgment. This work was funded by the Spanish Ministry of Education and Culture (project PB97-0547) and by the Xunta de Galicia (Infraestructura program).

References and Notes

(1) Formosinho, S. J.; Arnaut, L. G. *J. Photochem. Photobiol. A: Chem.* **1993**, *75*, 21.
(2) Ormson, S. M.; Brown, R. G. *Prog. React. Kinet.* **1994**, *19*, 45.
(3) Le Gourrierec, D.; Ormson, S. M.; Brown, R. G. *Prog. React. Kinet.* **1994**, *19*, 211.
(4) Kasha, M. *J. Chem. Soc., Faraday Trans. 2* **1986**, *82*, 2379.
(5) Taylor, C. A.; El-Bayoumi, M. A.; Kasha, M. *Proc. Natl. Acad. Sci. U.S.A.* **1969**, *63*, 253.
(6) McMorrow, D.; Aartsma, T. *Chem. Phys. Lett.* **1986**, *125*, 581.
(7) Moog, R. S.; Maroncelli, M. *J. Phys. Chem.* **1991**, *95*, 10359.
(8) Chapman, C. F.; Maroncelli, M. *J. Phys. Chem.* **1992**, *96*, 8430.
(9) Chen, Y.; Gai, F.; Petrich, J. W. *J. Am. Chem. Soc.* **1993**, *115*, 10158.
(10) Chou, P.-T.; Martinez, M. L.; Cooper, W. C.; McMorrow, D.; Collins, S.; Kasha, M. *J. Phys. Chem.* **1992**, *96*, 5203.
(11) Moog, R. S.; Bovino, S. C.; Simon, J. D. *J. Phys. Chem.* **1988**, *92*, 6545.
(12) Konijnenberg, A.; Huizer, A. H.; Varma, C. A. G. O. *J. Chem. Soc., Faraday Trans. 2* **1988**, *84*, 1163.
(13) Chang, C.-P.; Wen-Chi, H.; Meng-Shin, K.; Chou, P.-T.; Clements, J. H. *J. Phys. Chem.* **1994**, *98*, 8801.
(14) Mente, S.; Maroncelli, M. *J. Phys. Chem. A* **1998**, *102*, 3860.
(15) Folmer, D. E.; Wisniewski, E. S.; Hurley, S. M.; Castleman, A. W., Jr. *Proc. Natl. Acad. Sci. U.S.A.* **1999**, *96*, 12980.
(16) Folmer, D. E.; Wisniewski, E. S.; Stairs, J. R.; Castleman, A. W., Jr. *J. Phys. Chem. A* **2000**, *104*, 10545.
(17) Kyrychenko, A.; Stepanenko, Y.; Waluk, J. *J. Phys. Chem. A* **2000**, *104*, 9542.
(18) Waluk, J.; Komorowski, S. J.; Herbich, J. *J. Phys. Chem.* **1986**, *90*, 3868.
(19) Kyrychenko, A.; Herbich, J.; Izydorzak, M.; Wu, F.; Thummel, R. P.; Waluk, J. *J. Am. Chem. Soc.* **1999**, *121*, 11179.
(20) Marks, D.; Zhang, H.; Borowicz, P.; Waluk, J.; Glasbeek, M. *J. Phys. Chem. A* **2000**, *104*, 7167.
(21) Herbich, J.; Dobkowski, J.; Thummel, P.; Hegde, V.; Waluk, J. *J. Phys. Chem. A* **1997**, *101*, 5839.
(22) Dobkowski, J.; Herbich, J.; Galievsky, V.; Thummel, R. P.; Wu, F.; Waluk, J. *Ber. Bunsen-Ges.* **1998**, *102*, 469.
(23) Herbich, J.; Rettig, W.; Thummel, R. P.; Waluk, J. *Chem. Phys. Lett.* **1992**, *195*, 556.
(24) Herbich, J.; Waluk, J.; Thummel, R. P.; Hung, C.-Y. *J. Photochem. Photobiol. A.* **1994**, *80*, 157.
(25) Herbich, J.; Hung, C.-H.; Thummel, R. P.; Waluk, J. *J. Am. Chem. Soc.* **1996**, *118*, 3508.
(26) Kondo, M. *Bull. Chem. Soc. Jpn.* **1978**, *51*, 3027.
(27) Brown, R. G.; Entwistle, N.; Hepworth, J. D.; Hodgson, K. W.; May, B. *J. Phys. Chem.* **1982**, *86*, 2418.
(28) Rodríguez-Prieto, F.; Mosquera, M.; Novo, M. *J. Phys. Chem.* **1990**, *94*, 8536.
(29) Chang, C.-P.; Shabestary, N.; El-Bayoumi, M. A. *Chem. Phys. Lett.* **1980**, *75*, 107.
(30) Fuke, K.; Tsukamoto, K.; Misaizu, F.; Kaya, K. *J. Chem. Phys.* **1991**, *95*, 4074.
(31) Ingham, K. C.; Abu-Elgheit, M.; El-Bayoumi, M. A. *J. Am. Chem. Soc.* **1971**, *93*, 5023.
(32) Takeuchi, S.; Tahara, T. *J. Phys. Chem. A* **1998**, *102*, 7740.
(33) Chachisvilis, M.; Fiebig, T.; Douhal, A.; Zewail, A. H. *J. Phys. Chem. A.* **1998**, *102*, 669.
(34) Hetherington, W. M., III; Micheels, R. H.; Eisenthal, K. B. *Chem. Phys. Lett*. **1979**, *66*, 230.
(35) Fiebig, T.; Chachisvilis, M.; Manger, M.; Zewail, A. H.; Douhal, A.; Garcia-Ochoa, I.; de la Hoz Ayuso, A. *J. Phys. Chem. A* **1999**, *103*, 7419.
(36) Guallar, V.; Batista, V. S.; Miller, W. H. *J. Chem. Phys.* **1999**, *110*, 9922.
(37) Ríos Rodríguez, M. C.; Penedo, J. C.; Willemse, R. J.; Mosquera, M.; Rodríguez-Prieto, F. *J. Phys. Chem. A* **1999**, *103*, 7236.
(38) Mosquera, M.; Ríos Rodríguez, M. C.; Rodríguez-Prieto, F. *J. Phys. Chem. A* **1997**, *101*, 2766.
(39) Ríos Rodriguez, M. C.; Rodríguez-Prieto, F.; Mosquera, M. *Phys. Chem. Chem. Phys.* **1999**, *1*, 253.
(40) Melhuish, W. H. *J. Phys. Chem.* **1961**, *65*, 229.
(41) Demas, J. N.; Crosby, G. A. *J. Phys. Chem.* **1971**, *75*, 991.
(42) Rodríguez-Prieto, F.; Ríos Rodríguez, M. C.; Mosquera González, M.; Ríos Fernández, M. A. *J. Phys. Chem.* **1994**, *98*, 8666.
(43) Mosquera, M.; Penedo, J. C.; Ríos Rodríguez, M. C.; Rodríguez-Prieto, F. *J. Phys. Chem.* **1996**, *100*, 5398.
(44) Friedrich, D. M.; Wang, Z.; Joly, A. G.; Peterson, K. A.; Callis, P. R. *J. Phys. Chem. A* **1999**, *103*, 9644.
(45) Martin, D.; Weise, A.; Niclas, H.-J. *Angew. Chem., Int. Ed. Engl.* **1967**, *6*, 318.
(46) Reichardt, C. *Solvents and Solvent Effects in Organic Chemistry*, 2nd ed.; VCH: Weinheim, 1988.
(47) Catalán, J.; Mena, E.; Fabero, F.; Amat-Guerri, F. *J. Chem. Phys.* **1992**, *96*, 2005.
(48) Amat-Guerri, F.; Catalán, J.; Mena, E.; Fabero, F. *Magn. Reson. Chem.* **1992**, *30*, 800.
(49) Catalán, J.; de Paz, J. L. G.; del Valle, J. C.; Kasha, M. *J. Phys. Chem. A* **1997**, *101*, 5284.
(50) Rodríguez-Prieto, F.; Penedo, J. C.; Mosquera, M. *J. Chem. Soc., Faraday Trans.* **1998**, *94*, 2775.
(51) Demas, J. N. *Excited-State Lifetime Measurements*; Academic Press: New York, 1983.
(52) Penedo, J. C. Ph.D. Thesis, University of Santiago de Compostela, Spain, 1998.
(53) del Valle, J. C.; Domínguez, E.; Kasha, M. *J. Phys. Chem. A* **1999**, *103*, 2467.